

Structure, magnetism and absorption spectra of some orthouranates and orthoneptunates

M. Bickel*, B. Kanellakopoulos and B. Powietzka

Institut für Heiße Chemie, Kernforschungszentrum Karlsruhe, Karlsruhe (Germany)

(Received January 22, 1992)

Abstract

The crystallographic and spectroscopic properties as well as the magnetic susceptibilities of Sr_3UO_6 , Ca_3UO_6 , Sr_3NpO_6 and Ca_3NpO_6 were determined. Data for the uranates are in agreement with structures proposed earlier. From X-ray powder patterns and IR arguments the neptunates seem to exhibit a somewhat less distorted lattice. Electronic spectra indicate only slightly distorted NpO_6 octahedra. Magnetic susceptibilities are comparable with data from other $5f^0$ and $5f^1$ systems respectively. The absence of magnetic transitions in the neptunates is explained by the unavailability of An–O–An chains in the lattice, thus suppressing superexchange via oxygen ions.

1. Introduction

Ternary oxides containing $5f$ ions with an odd number of f electrons and a related magnetic ground state often order magnetically at low temperatures [1–13]. While the main ordering mechanism mostly can be explained in a qualitative way by superexchange via oxygen ions, there exists very little information about the details of such magnetic transitions. Thus, during recent years we began to investigate ternary oxides of Np(VI) with the $[\text{Rn}]5f^1$ electronic configuration to study relationships between crystal structures and magnetic properties of these compounds.

In the course of these studies our interest was focused on the “orthoactinidates” with the general formula $\text{M}^{\text{II}}_3\text{AnO}_6$. These compounds contain hexavalent actinide central ions in a more or less distorted coordination octahedron of oxygen ions. The crystal structure is a perovskite superstructure; this can be emphasized by writing the formula in a more “perovskite-like” (ABO_3) way as $\text{M}^{\text{II}}(\text{M}^{\text{VI}}_{0.5}\text{M}^{\text{VI}}_{0.5})\text{O}_3$. The ideal, cubic structure is shown in Fig. 1. From there it is obvious that the M^{II} ion exhibits two different coordination numbers (KZ) in the crystal, indicating already that the number of stable cubic compounds of this type must be very limited. Indeed, only a few

*Author to whom correspondence should be addressed. Present address: CBNM, Steenweg op Retie, B-2440 Geel, Belgium.

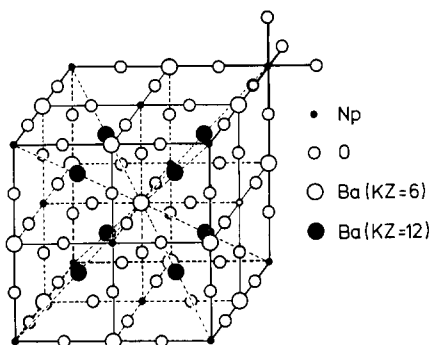


Fig. 1. Ideal, cubic perovskite superstructure.

representatives of the cubic type exist [14, 15], because the octahedral interstices formed by M^{2+} and O^{2-} in the closest packing usually are too small for M^{2+} itself. Replacing one-third of M^{2+} with a smaller M^{*2+} makes the cubic structure much more likely [16–19].

From their structure one would not expect these kinds of compounds to exhibit magnetic ordering at low temperatures because on one hand the distances between the paramagnetic centres are relatively long and on the other $M-O-M$ chains are interrupted by diamagnetic ions which should suppress superexchange interactions. Considerable disagreement about the structure exists in the literature and we hoped to obtain a closer insight into the An^{6+} site symmetry by using different physical methods of investigation for these compounds.

2. Experimental details

The samples were prepared by thermal treatment of a mixture of alkaline earth carbonate with U_3O_8 or NpO_2 . The starting materials $BaCO_3$ and $CaCO_3$ (p.a., Merck, Darmstadt, FRG), $SrCO_3$ (Optipur, Merck), U_3O_8 (prepared by the heating in air of UO_2 , nuclearrein, Merck, Darmstadt, FRG) and NpO_2 (spectroscopically analysed, ORNL) were dried at 300 °C for 16 h directly before use. They were then ground together in an agate mortar for at least 15 min and the finely powdered, homogeneous-looking mixture was put into the furnace in a corundum boat. The reaction took place in a quartz tube at 1000–1200 °C under a stream of oxygen. After approximately 12 h the product was reground and again left under the same conditions for another 12 h. The resulting compound was quenched to room temperature and stored under dry oxygen. Sr_3UO_6 , Sr_3NpO_6 , Ca_3UO_6 and Ca_3NpO_6 were prepared by this method.

The samples were characterized by X-ray diffraction (Debye–Scherrer) using nickel-filtered $Cu K\alpha$ radiation. IR spectra of the compounds pressed as KBr and polyethylene pellets were recorded with a Perkin–Elmer M283

spectrometer ($4000\text{--}200\text{ cm}^{-1}$) and a Beckman FS 720 interferometer ($40\text{--}400\text{ cm}^{-1}$) respectively. Electronic spectra of the substances pressed as KBr pellets were taken between 400 and 1400 nm with a Cary 17 spectrophotometer at 77 K. Measurements of the magnetic susceptibility from room temperature down to 1.3 K were performed with a Faraday balance, the details of which are described elsewhere [1, 10].

3. Results

3.1. X-ray diffraction

The powder patterns of Ca_3UO_6 and Sr_3UO_6 were indexed in a monoclinic symmetry in agreement with X-ray and neutron data from Loopstra and Rietveld [20]. In the patterns of Ca_3NpO_6 and Sr_3NpO_6 no indication of a line splitting leading to a monoclinic structure could be found; hence, they were indexed in an orthorhombic symmetry. The lattice constants obtained are listed in Table 1 in comparison with literature values.

3.2. IR spectroscopy

The IR and far-IR spectra of Sr_3UO_6 and Ca_3UO_6 are shown in Figs. 2 and 3 respectively. Spectra of the corresponding neptunium compounds can be seen in Fig. 4 in comparison with their uranium homologues. The transition energies are listed in Table 2, together with a proposed assignment.

3.3. Electronic spectroscopy

From comparison with other ternary neptunium oxides with similar coordinations, particularly with Ba_3NpO_6 [2], the electronic transitions of

TABLE 1
Lattice constants of orthouranates and orthoneptunates

Compound	Lattice constants	
	This work	Literature [20]
Ca_3UO_6	$a = 569.9\text{ pm}$ $b = 593.8\text{ pm}$ $c = 830.6\text{ pm}$ $\beta = 90.7^\circ$	$a = 572.75\text{ pm}$ $b = 595.64\text{ pm}$ $c = 829.82\text{ pm}$ $\beta = 90.568^\circ$
Sr_3UO_6	$a = 597.3\text{ pm}$ $b = 621.8\text{ pm}$ $c = 852.1\text{ pm}$ $\beta = 90.7^\circ$	$a = 595.88\text{ pm}$ $b = 617.95\text{ pm}$ $c = 855.35\text{ pm}$ $\beta = 90.192^\circ$
Ca_3NpO_6	$a = 569.0\text{ pm}$ $b = 593.8\text{ pm}$ $c = 819.3\text{ pm}$	
Sr_3NpO_6	$a = 593.2\text{ pm}$ $b = 619.5\text{ pm}$ $c = 853.2\text{ pm}$	

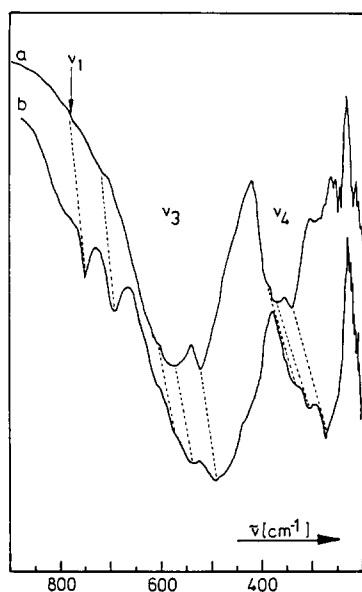


Fig. 2. IR spectra of Ca_3UO_6 (spectrum a) and Sr_3UO_6 (spectrum b).

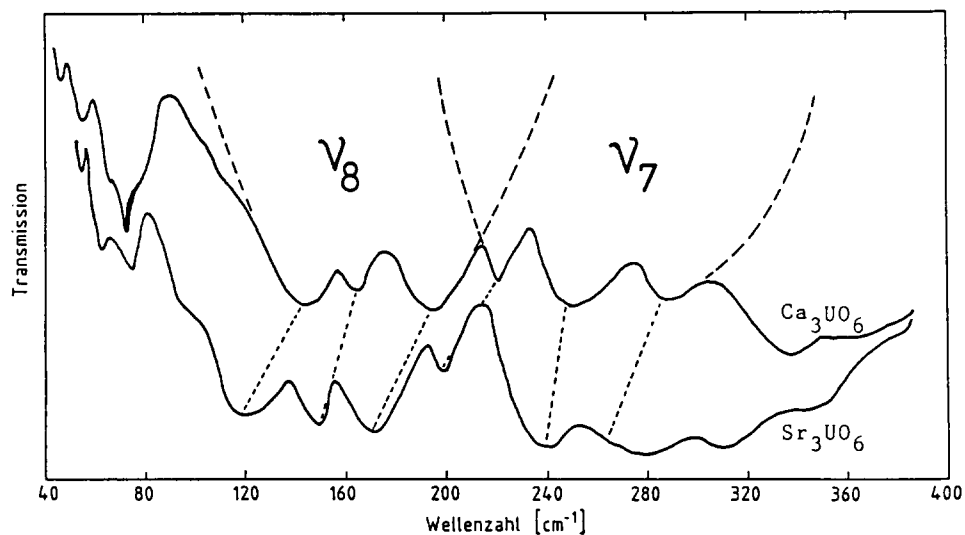


Fig. 3. Far-IR spectra of Ca_3UO_6 and Sr_3UO_6 .

$\text{M}^{\text{II}}_3\text{NpO}_6$ can be expected in the near-IR region [1, 2, 10–13]. Indeed, two transition bands and a shoulder on the charge transfer rise can be observed in the spectra (Fig. 5). The proposed assignment of the corresponding energies is given in Table 3 together with literature data for the barium compound.



Fig. 4. IR spectra of Sr_3NpO_6 (spectrum a), Sr_3UO_6 (spectrum b), Ca_3NpO_6 (spectrum c) and Ca_3UO_6 (spectrum d).

TABLE 2

IR bands of the orthoactinidates

Vibration	Sr_3UO_6 (cm^{-1})	SrNpO_6 (cm^{-1})	Ca_3UO_6 (cm^{-1})	Ca_3NO_6 (cm^{-1})
ν_1	750	— ^a	750–770	— ^a
ν_3	492	515	523	534
	535	550	573	570
	600	615	610	610
ν_4	275	297	335	345
	310	320	372	375
	348	350	390	395
ν_7	260	272	290	310
	238	260	250	298
	200	— ^b	220	270
ν_8	170	— ^b	194	— ^b
	148	— ^b	164	— ^b
	120	— ^b	144	— ^b

^aRaman active not observed.

^bNo far-IR spectra ($\nu < 200 \text{ cm}^{-1}$) of the neptunates were recorded.

3.4. Susceptibility measurements

Sr_3UO_6 and Ca_3UO_6 , as expected, exhibit temperature-independent, weakly paramagnetic susceptibilities of $(158 \pm 0.5) \times 10^{-6} \text{ cm}^3 \text{ mol}^{-1}$ and

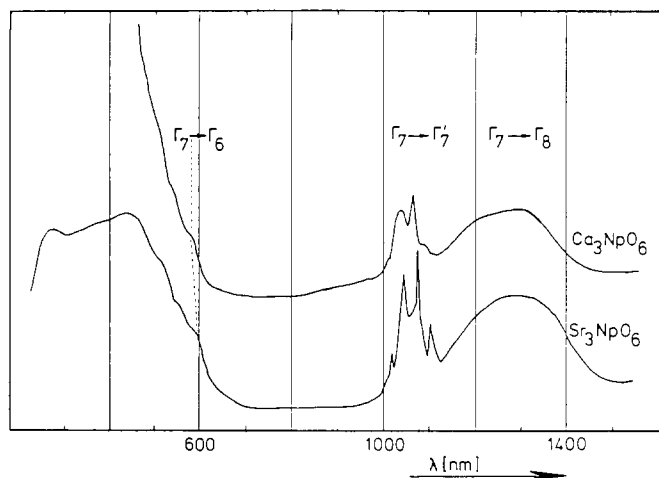


Fig. 5. Electronic spectra of Sr_3NpO_6 and Ca_3NpO_6 .

TABLE 3

Assignment of the electronic spectra of Ba_3NpO_6 , Sr_3NpO_6 and Ca_3NpO_6

Transition	Energy (cm^{-1})			
	Ba_3NpO_6 [2]		Sr_3NpO_6	Ca_3NpO_6
	Calculated	Observed		
$\Gamma_7 \rightarrow \Gamma_8$	8000	7690	7605	7692
$\Gamma_7 \rightarrow \Gamma_7'$	9390	9390	9442	9483
$\Gamma_7 \rightarrow \Gamma_8'$	13729	11760		
$\Gamma_7 \rightarrow \Gamma_6$	16263	> 16500	17241	17391

$(156 \pm 0.5) \times 10^{-6} \text{ cm}^3 \text{ mol}^{-1}$ respectively over the entire temperature range investigated (77–300 K).

The neptunium compounds exhibit the paramagnetic behaviour of a $5f^1$ system in a distorted octahedral crystal field (Figs. 6 and 7), as already known from various other ternary neptunium oxides [1–13]. The Curie–Weiss law is not followed owing to a temperature-independent contribution to the susceptibility which can be evaluated by extrapolation of the data towards infinite temperature:

$$\text{Sr}_3\text{NpO}_6 \quad \chi_m^{\text{TIP}} = (283 \pm 2) \times 10^{-6} \text{ cm}^3 \text{ mol}^{-1}$$

$$\text{Ca}_3\text{NpO}_6 \quad \chi_m^{\text{TIP}} = (347 \pm 2) \times 10^{-6} \text{ cm}^3 \text{ mol}^{-1}$$

After correction of the measured data with respect to χ^{TIP} the susceptibilities of both substances follow a Curie–Weiss law with the following parameters:

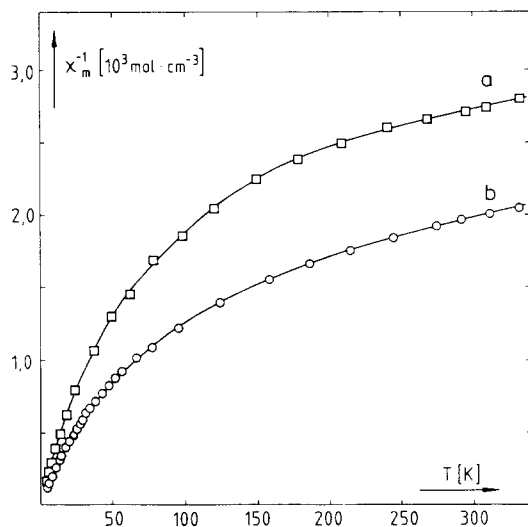


Fig. 6. Reciprocal molar susceptibility of Sr_3NpO_6 (curve a) and Ca_3NpO_6 (curve b) as a function of temperature.

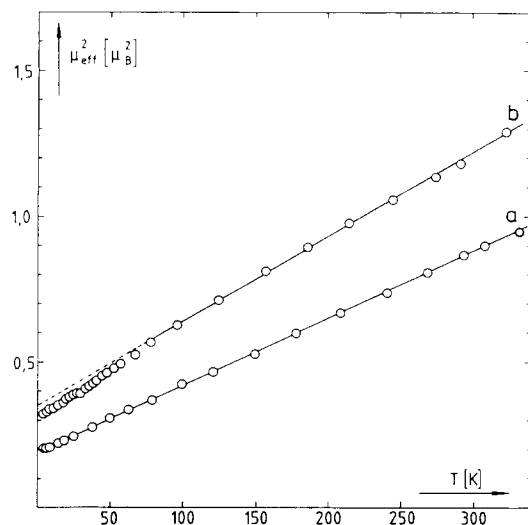


Fig. 7. Magnetic moments of Sr_3NpO_6 (curve a) and Ca_3NpO_6 (curve b) as a function of temperature.

Sr_3NpO_6 $C = (2.45 \pm 0.03) \times 10^{-2} \text{ mol cm}^{-3} \text{ K}^{-1}$; $\theta = 0 \pm 3 \text{ K}$

Ca_3NpO_6 $C = (4.74 \pm 0.03) \times 10^{-2} \text{ mol cm}^{-3} \text{ K}^{-1}$; $\theta = -4 \pm 3 \text{ K}$

For none of the compounds is an indication of magnetic ordering above 4.2 K observable.

4. Discussion

4.1. The crystal structures

The first structural investigations on this class of compounds took place in 1954–1955. Therein Ba_3UO_6 was indexed cubically, and the corresponding strontium and calcium compounds were described as distorted, but were not further explained [15, 21]. Russian researchers found the structures to be cubic (Ba_3UO_6) [22], pseudocubic (Sr_3UO_6) [23] and orthorhombic (Ca_3UO_6) [24]. The corresponding neptunates were synthesized by Keller in 1962. There a cubic structure was ascribed to Ba_3NpO_6 , and in the strontium and calcium cases distortions were found, but not further explained [25, 26].

Precise measurements using X-ray and neutron diffraction methods yielded a tetragonal structure for Ba_3UO_6 [27] and monoclinic structures for Sr_3UO_6 and Ca_3UO_6 [20]. The unit cell is shown idealized (orthorhombic) and distorted (monoclinic) in Fig. 8. A monoclinic symmetry has also been found by later researchers [28]. In some recent publications the neptunates were found to be not isomorphic with the corresponding uranates, but detailed information was not given [16, 29, 30].

In the present work agreement was found with the values of Loopstra and Rietveld [20] confirming the structures shown in Fig. 8 for the uranates, as well as the lattice constants (Table 1). In the case of the neptunates no line splitting indicating a monoclinic distortion could be found; hence, the patterns were indexed in an orthorhombic symmetry (Table 1).

These findings are confirmed by the interpretation of the IR data. Although the spectra here are much more complicated than, for example, those of the simple $\text{M}^{\text{II}}\text{An}^{\text{IV}}\text{O}_3$ perovskites, it can be shown that they are in agreement with the crystal structures described above.

A normal coordinate analysis for such systems was performed by Liegeois-Duyckaerts and Tarte [31], yielding ten modes of vibration for the cubic symmetry (Fig. 1):

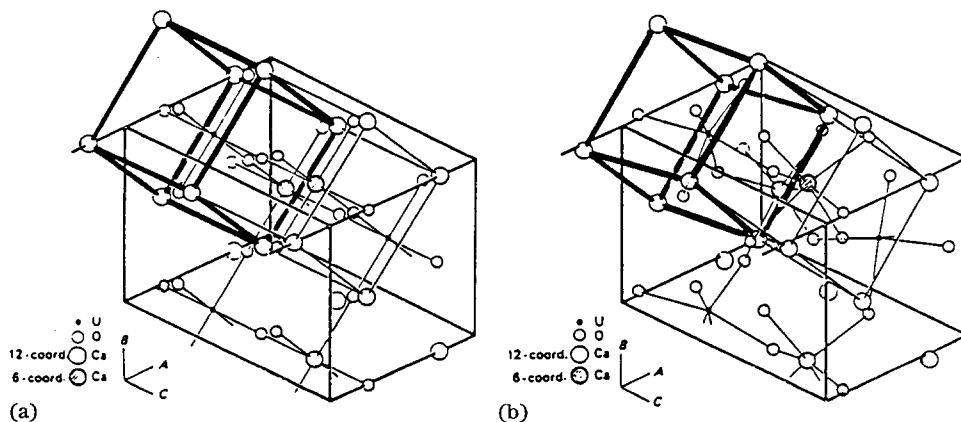


Fig. 8. (a) Idealized and (b) real structure of Ca_3UO_6 [27]. The perovskite unit is emphasized.

$A_{1g}(\nu_1), E_g(\nu_2), 2T_{2g}(\nu_5, \nu_9)$	Raman active
$4T_{1u}(\nu_3, \nu_4, \nu_7, \nu_8)$	IR active
$T_{1g}(\nu_6), T_{2u}(\nu_{10})$	inactive

This nomenclature (ν_1 – ν_{10}) is connected with the distinction between “internal” and “external” vibrations according to Last [32], *i.e.* ν_1 – ν_5 are internal vibrations of the MO_6 octahedron, and ν_7 – ν_{10} are external lattice vibrations. Because of the expected strong coupling between the internal and external modes, this distinction is not really justified in the present case; nevertheless, it is helpful for interpretation and therefore will be used throughout the text.

In the IR spectra (Fig. 2) the two internal modes of the AnO_6 octahedron, ν_3 and ν_4 , are clearly recognizable. They are threefold split, *i.e.* their degeneracy is removed; hence, the maximum possible symmetry is orthorhombic. Furthermore, the Raman-active mode ν_1 is observed as a shoulder in Ca_3UO_6 and as a low intensity peak in Sr_3UO_6 . This corresponds to a removal of the Raman–IR alternative rule and hence to a loss of the symmetry centre. Therefore, the symmetry must be lower than orthorhombic. A further band appearing in the spectra can be assigned to a combination of ν_3 and ν_7 .

In the far-IR spectra the two lattice modes ν_7 and ν_8 are observed. They also are split threefold, according to the crystal symmetry (Fig. 3). A proposed assignment of all vibration bands is given in Table 2.

Generally all bands of Sr_3UO_6 are shifted to lower energies with respect to those of Ca_3UO_6 ; this is expected because of the smaller mass of calcium compared with strontium.

The IR spectra of the neptunates are very similar to those of the corresponding uranates. The important difference is the absence of the Raman-active ν_1 in Sr_3NpO_6 , which indicates a higher symmetry than in Sr_3UO_6 . Again this result is in agreement with the X-ray diffraction results: no monoclinic line splitting was observed in the neptunates.

The assignment of the absorption bands was followed through in analogy to the uranates and is also listed in Table 2. Generally, the bands of the neptunates are shifted slightly to higher energies with respect to the uranates owing to the lower mass of neptunium compared with uranium.

4.2. The electronic spectra

The Np^{6+} ion has the $[Rn]5f^1$ electronic configuration with a ${}^2F_{5/2}$ ground state and a ${}^2F_{7/2}$ first excited state. In an octahedral crystal field these terms undergo a splitting according to the level scheme in Fig. 9. Although the overall crystal structure is orthorhombic in the compounds under investigation, the distortion of the NpO_6 octahedron itself is relatively small (Fig. 6); hence, one would not expect very large deviations from the level scheme of Fig. 9.

The assignment of the spectrum was performed according to the assignment of Ba_3NpO_6 . As mentioned before, this compound is of very similar structure (concerning the NpO_6 octahedron) and therefore can be expected to exhibit a similar absorption spectrum. Its bands had been fitted with a

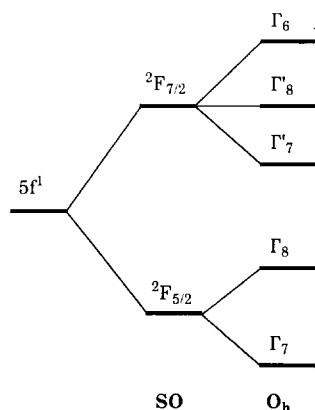


Fig. 9. Spin-orbit and crystal field splitting in an octahedral field.

model using the cubic crystal field parameters Δ and θ , the spin-orbit coupling constant ζ and two orbital reduction factors k and k' to take into account effects of covalency [1, 2]. If the coordination polyhedra are similar in Ba_3NpO_6 , Sr_3NpO_6 and Ca_3NpO_6 , the above parameters should also be similar and therefore the transitions should occur at similar energies.

Indeed, this is the case, as can be seen from Table 3, where the transition energies of Sr_3NpO_6 and Ca_3NpO_6 are compared with observed and calculated values of Ba_3NpO_6 from ref. 2. The $\Gamma_7 \rightarrow \Gamma'_8$ transition was not observed in the strontium and calcium compounds; in the barium compound this band also had a very low intensity.

Again, these results are in agreement with the above-suggested crystal structures, *i.e.* slightly distorted NpO_6 octahedra in a crystal of relatively low symmetry.

4.3. The magnetic susceptibility

Since the magnetic susceptibility reflects the occupation of the electronic levels, which is very similar in Ba_3NpO_6 , Sr_3NpO_6 and Ca_3NpO_6 as has been pointed out above, one does not expect large differences in magnetic behaviour among these compounds.

This is indeed the case as can be seen in Figs. 6 and 7 and from comparison with the Ba_3NpO_6 data from refs. 1 and 2. The dependence of the susceptibilities on temperature exhibits a Curie-Weiss behaviour with the addition of a temperature-independent paramagnetism. At high temperatures this behaviour is very similar to practically all ternary Np^{VI} oxides containing NpO_6 octahedra investigated so far [1-13], the room temperature values of which lie in the range $(460 \pm 90) \times 10^6 \text{ cm}^3 \text{ mol}^{-1}$. The extrapolated temperature-independent susceptibility of Ca_3NpO_6 lies in the middle region of the temperature-independent paramagnetic susceptibilities of the hitherto investigated ternary oxides with an Np^{VI} central ion, ranging from 283×10^{-6}

to $389 \times 10^{-6} \text{ cm}^3 \text{ mol}^{-1}$ [10]. In contrast, the strontium compound exhibits the lowest value found so far.

In contrast to several Np^{VI} ternary oxides no magnetic transition is observable. This fact is consistent with the values for the Weiss constants of practically zero indicating only very small, if any, interactions present between the paramagnetic centres.

Usually in this class of compounds the ordering phenomena are explained by a superexchange mechanism via the oxygen ions. To make this possible, An–O–An chains must be present in the crystal, which here is not the case. Therefore it is not surprising that no magnetic ordering occurs, because the An–An distances are far too large for dipole ordering above 4 K.

From this statement one would conclude that magnetic ordering should become possible if the diamagnetic ions that “insulate” the NpO_6 octahedra are exchanged with paramagnetic ions. This, indeed, occurs, as can be seen from the compounds $\text{Ba}_2\text{MnNpO}_6$ and $\text{Ba}_2\text{FeNpO}_6$. Here the NpO_6 octahedra are “bridged” by paramagnetic Mn^{2+} or Fe^{2+} ions; the result is magnetic ordering at 65 K and 200 K respectively [33].

5. Conclusions

The crystal structures of Sr_3UO_6 and Ca_3UO_6 determined earlier have been confirmed by X-ray diffraction and IR spectroscopic methods. The corresponding neptunium compounds exhibit a different structure of higher symmetry. Although the lattice symmetry in all compounds is rather low (orthorhombic or monoclinic), the symmetry of the actinide coordination polyhedron does not seem to be strongly affected, since an octahedral crystal field model is able to explain the observed electronic transitions. It is unlikely that the AnO_6 octahedron is ideal, but the distortions are much weaker than in, for example, Na_4NpO_5 or Na_2NpO_4 , where a tetragonal crystal field model is necessary to explain the spectra [2, 13].

The magnetic measurements are also in agreement with a slightly distorted NpO_6 octahedron, although the magnetic susceptibility does not seem to be extremely sensitive to slight changes in symmetry and bond lengths in these compounds as long as the main coordination feature, the AnO_6 octahedron, is conserved [12].

The compounds do not order magnetically at low temperatures, which is to be expected from their crystal structures. An–An distances are too large to allow dipole interaction; superexchange is not possible because the neptunium–oxygen octahedra are separated by diamagnetic ions in all three lattice directions, *i.e.* only An–O–M–O–An chains exist where An–O–An chains would be necessary.

In Sr_3UO_6 and Ca_3UO_6 , as in all ternary oxides containing ions with the $[\text{Rn}]5f^0$ electronic configuration investigated so far, the $5f^0$ ion exhibits a weak, paramagnetic susceptibility. Since the ions do not contain f electrons

a significant degree of covalency seems to be present in the An–O bond of these oxides. This covalency is not surprising, when actinyl groups are a feature of the crystal lattice, but even in compounds with six almost equidistant oxygen ions in the coordination octahedron the susceptibilities lie in the same range. Thus, the influence of bonding electrons on the magnetic behaviour is not completely negligible in such systems.

The susceptibilities of Np^{VII} compounds are higher than those in iso-electronic U^{VI} compounds, which is consistent with the general observation that the tendency towards covalency increases with increasing oxidation state in the actinide series.

References

- 1 E. Henrich, *Dissertation*, University of Heidelberg, 1971.
- 2 B. Kanellakopulos, E. Henrich, C. Keller, F. Baumgärtner, E. König and V. P. Desai, *Chem. Phys.*, *53* (1980) 197.
- 3 C. Miyake, K. Fuji and S. Imoto, *Chem. Phys. Lett.*, *61* (1979) 124.
- 4 C. Miyake, H. Takeuchi, H. Ohya-Nishiguchi and S. Imoto, *Phys. Status Solidi*, *74* (1982) 17.
- 5 C. Miyake, K. Fuji and S. Imoto, *Chem. Phys. Lett.*, *46* (1977) 349.
- 6 J. Jové, F. Nectoux, A. Tabuteau and M. Pagés, *Proc. Conf. on the Application of the Mössbauer Effect*, in *Proc. Indian Natl. Sci. Acad., Part A*, *410* (1982) 580.
- 7 F. Nectoux, J. Jové, A. Cousson, M. Pagés and J. Gal, *J. Magn. Magn. Mater.*, *24* (1981) L113.
- 8 B. Kanellakopulos, C. Keller, R. Klenze and A. H. Stollenwerk, *Physica B*, *102* (1980) 221.
- 9 A. H. Stollenwerk, *Dissertation*, University of Heidelberg, 1979.
- 10 M. Bickel, *KfK Rep. 4109*, 1986, Kernforschungszentrum Karlsruhe.
- 11 M. Bickel, S. Geggus, H. Appel, H. Haffner and B. Kanellakopulos, *J. Less-Common Met.*, *121* (1986) 291.
- 12 A. Appel, M. Bickel, S. Melchior, B. Kanellakopulos and C. Keller, *J. Less-Common Met.*, *162* (1990) 323.
- 13 M. Bickel, B. Kanellakopulos and B. Powietzka, *J. Less-Common Met.*, *170* (1991) 161.
- 14 E. G. Steward and H. P. Rooksby, *Acta Crystallogr.*, *4* (1951) 503.
- 15 R. Scholder and L. Brixner, *Z. Naturforsch., Teil B*, *10* (1955) 178.
- 16 R. Gens, J. Fuger, L. R. Morss and C. W. Williams, *J. Chem. Thermodyn.*, *17* (1985) 561.
- 17 A. W. Sleight and R. Ward, *Inorg. Chem.*, *1* (1962) 790.
- 18 L. Katz and R. Ward, *Inorg. Chem.*, *1* (1964) 205.
- 19 G. Blasse, *J. Inorg. Nucl. Chem.*, *27* (1965) 993.
- 20 B. O. Loopstra and H. M. Rietveld, *Acta Crystallogr. Sect. B*, *25* (1969) 787.
- 21 W. Rüdorff and F. Pfitzner, *Z. Naturforsch., Teil B*, *9* (1954) 568.
- 22 E. A. Ippolitova, I. A. Bereznikova, V. Y. Leanidov and C. M. Kovba, *ANL Trans.*, *33* (1961) 186.
- 23 E. A. Ippolitova, I. A. Bereznikova, V. D. Kosynkin, Y. P. Simanov and L. M. Kovba, *ANL Trans.*, *33* (1961) 180.
- 24 I. A. Bereznikova, E. A. Ippolitova, Y. P. Simanov and L. M. Kovba, *ANL Trans.*, *33* (1961) 176.
- 25 C. Keller, *KfK Rep. 225*, 1964, Kernforschungszentrum Karlsruhe.
- 26 C. Keller, *Nukleonik*, *5* (1963) 7.
- 27 H. M. Rietveld, *Acta Crystallogr.*, *20* (1966) 508.
- 28 S. Kemmler-Sack and I. Seemann, *Z. Anorg. Allg. Chem.*, *411* (1975) 61.
- 29 L. R. Morss, J. Fuger and H. D. B. Jenkins, *J. Chem. Thermodyn.*, *14* (1982) 377.

- 30 L. R. Morss, C. W. Williams, I. K. Choi, R. Gens and J. Fuger, *J. Chem. Thermodyn.*, *15* (1983) 1093.
- 31 M. Liegeois-Duyckaerts and P. Tarte, *Spectrochim. Acta A*, *30* (1974) 1771.
- 32 J. T. Last, *Phys. Rev.*, *105* (1957) 1740.
- 33 E. Simoni, H. Abazli, A. Cousson and M. Pagés, *Radiochem. Radioanal. Lett.*, *49* (1981) 37.